# A Dual Six-Port Automatic Network Analyzer and Its Performance

NAK SAM CHUNG, MEMBER, IEEE, JEONG HWAN KIM, AND JOON SHIN

*Abstract*—**A computer-controlled six-port automatic network analyzer (ANA) capable of measuring complex reflection coefficients of one-port devices, effective efficiencies of power sensors, and $S$-parameters of two-port devices over 2–18 GHz is described. System calibration based on the TRL technique is discussed and performance tests on measuring effective efficiencies, reflection coefficients, and $S$-parameters are summarized.**

## I. Introduction

SINCE HOER AND ENGEN introduced the six-port concept in 1972, a considerable amount of theoretical work has been done, and a number of six-port systems have been implemented and have demonstrated good performance [1]–[5].

As seen from the studies made so far, six-ports are inherently simple and stable devices which do not need to be constructed of precision components, and require only power information in order to measure complex impedances—a convenient alternative to conventional network analyzers which have much electronic complexity. Six-port automatic network analyzers (ANA) cover a wide frequency range, save much time in measurement, and are, at least in principle, capable of returning error-free results after a suitable calibration procedure has been implemented.

At the Korea Standards Research Institute (KSRI), we have a plan to set up versatile dual six-port ANA's to meet most of the microwave measurement needs. Hopefully, they will also cover most of the waveguide devices by simply using coaxial-to-waveguide adaptors.

The first system completed is a dual six-port ANA for the frequency range 2–18 GHz. The system is capable of measuring complex reflection coefficients of one-port devices, effective efficiencies of power sensors, and $S$-parameters of two-port devices. In this paper, the hardware configuration of the system, as well as some results of the performance test, will be described.

## II. System Description

The six-port itself uses the configuration originally designed by Engen, which is shown in Fig. 1. Here "$Q$" and "$D$" represent, respectively, a quadrature hybrid and a power divider. The 3.5-mm semirigid cable and SMA connectors have been used for the interconnection between components. The RF input port, measurement port, and remaining four ports terminated by power detectors use type-$N$ connectors. Assuming ideal components and lossless lines in the configuration, the wave amplitudes at the detector ports are as shown in Fig. 1. The $q$-points are $q_3 = j$, $q_5 = -(1+j)$, $q_6 = 1-j$, so that $|q_3| = 1$, $|q_5| = |q_6| = \sqrt{2}$, and their phase spacing is 135°–90°–135° [1].

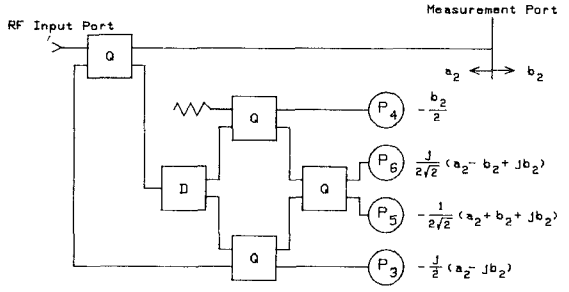


Fig. 1. Six-port configuration. "$Q$" and "$D$" represent a quadrature hybrid and a power divider, respectively.

Fig. 2 is a block diagram of the dual six-port ANA. All instruments are under the control of an HP 9845B desktop computer via the IEEE-488 standard interface bus.

A microwave synthesizer is used for the RF source, and its frequency can be varied under computer control in 1-MHz steps and its output level up to 13 dBm in 1-dB steps. In order to provide the desired power at the measurement port, a programmable power supply (D/A converter) is used to supply precise offset voltage to the automatic level control loop of the synthesizer for fine control of the output level.

To meet the need for high-level RF drive to the six-port, three traveling-wave tube amplifiers (TWTA) are used to amplify the output of the synthesizer. The amplified RF signal is passed through a filter box comprised of four low-pass filters and one bandpass filter to reduce harmonics and subharmonics.

Four 1P6T switches are used to select the appropriate TWTA and filter as required by the frequency of the RF signal. The dividing circuit before the six-port sensors is used for providing phase differences of 90°, 180°, 270°, and 0° between the RF signals applied to six-port #1 and six-port #2.

Manuscript received April 20, 1984; revised July 30, 1984. This work was supported in part by the Ministry of Science and Technology, Republic of Korea, under the Development of Automation Technology for Precision Measurement project, 1982–1983.

The authors are with the Korea Standards Research Institute, Taedok Science Town, Republic of Korea.

0018-9480/84/1200-1683$01.00 ©1984 IEEE

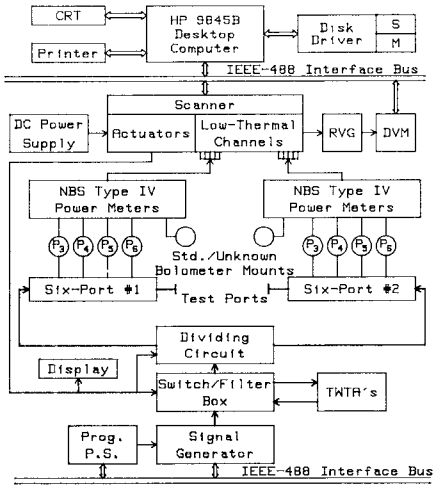


Fig. 2. Block diagram of the dual six-port ANA.

Each six-port has four sidearm ports terminated by thermistor mounts and these thermistor mounts are housed in an aluminium block whose temperature is maintained constant by a temperature controller. This eliminates the effect of environmental temperature changes on the thermistor mounts. Each thermistor mount, in turn, is connected to an NBS Type IV power meter and the resulting dc output is routed through a low thermal channel of a scanner and connected in series with a precision dc reference voltage generator (RVG) to a DVM, so that the DVM reads the difference between the dc output of the power meter and the RVG output. This is done so that the DVM remains on its lowest range with the best resolution of 1 $\mu$V.

A display panel is constructed to show the RF signal path, operating conditions of TWTA's and switches, and the phase difference between the RF signals applied to six-ports #1 and #2.

## III. Calibration and Software

The technique used to calibrate the dual six-port ANA is based on the "Thru-Reflect-Line" (TRL) technique [2] and the calibration procedure is composed of the following six steps.

1) With a calibrated thermistor mount connected to measurement port #1, the sidearm power readings of the six-port #1, and the power reading of the measurement port are recorded.

2) A nominal 10-dB pad of unknown attenuation is inserted between six-ports #1 and #2, and all sidearm power readings are recorded for the four different settings of the dividing circuit (0°, 90°, 180°, and 270°).

3) A precision reference line of unknown length is inserted, and all sidearm power readings are recorded for the four different settings of the dividing circuit as in step 2) (Line).

4) If the connectors are sexless, a highly reflecting termination (a nominal short) of unknown $\Gamma$ is connected first to one of the measurement ports and then the other. In each connection, the corresponding sidearm power readings are recorded (Reflect).

If the connectors are not sexless, two highly reflecting terminations (nominal shorts) of unknown $\Gamma$ (they are assumed to have the same $\Gamma$) are connected to measurement ports #1 and #2, and all sidearm power readings are recorded.

5) With measurement ports #1 and #2 open, all sidearm power readings are recorded.

6) Finally, with the measurement ports connected together, all sidearm power readings are recorded for the four different settings of the dividing circuit as in step 2) (Thru).

With all power readings obtained with the above procedure, the six-port to four-port reduction [2], [3] is performed and the TRL solution is obtained at each frequency by a BASIC program.

Step 1) is done for obtaining a constant needed for power measurement [2], steps 3), 4), and 6) for getting the TRL solution, and the remaining steps for providing redundancies to increase the accuracy of calibration constants and for providing check standards [5]. Three-port calibration constants needed for measuring $S$-parameters of nonreciprocal two-port devices are also obtained [4].

For power measurement, the system response is observed with two calibrated thermistor mounts connected to the measurement port.

The net power delivered to the bolometer mount can be written as follows [2]:

$$P_{\text{net}} = \frac{P_b}{\eta} = KP_g \tag{1}$$

where $\eta$ is the effective efficiency of the bolometer mount, $P_b$ is the substituted dc power in the bolometer, $K$ is a constant determined only by six-port calibration constants and is obtained from the calibration step 1), and $P_g$ is a real factor determined by six-port calibration constants and the reflection coefficient of the bolometer mount.

From (1), it can be shown that the following relation is valid:

$$\eta_u = \eta_s \frac{P_{bu}P_{gs}}{P_{bs}P_{gu}} \tag{2}$$

where the subscripts $u$ and $s$ indicate the unknown and standard bolometer mounts, respectively. Here $P_{bu}$ and $P_{bs}$ are measured directly by using the NBS Type IV power meters, and $P_{gs}$ and $P_{gu}$ are calculated in the six-port to four-port reduction.

## IV. Performance

An evaluation of the system performance revealed a system malfunction above 17.5 GHz due to two $q$-points getting closer to each other. Evaluation of short-term stability and long-term stability has not been done at this time.

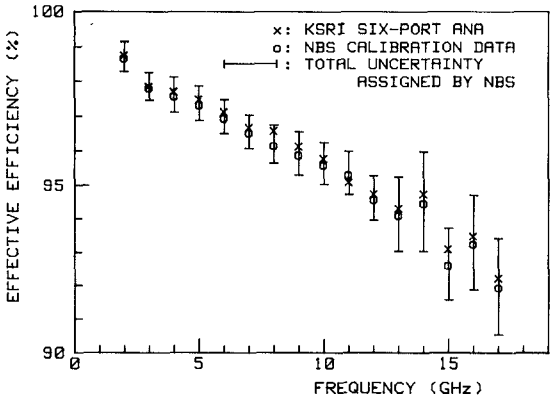


Fig. 3. Performance in measuring effective efficiency of a bolometer.

For all the results to be discussed below, we calibrated the system five times in 1-GHz steps over the 2–17-GHz range, and the necessary measurements were made each time.

To evaluate the system accuracy in transferring the effective efficiencies of bolometers, we measured the effective efficiency of a thermistor mount which had been calibrated by NBS. As shown in Fig. 3, where the average values of the five measurements are compared with the NBS calibration data, the measured effective efficiencies agree with NBS calibration data within the total uncertainty assigned by NBS. The imprecision or the standard deviation of the five measurements is approximately an order of magnitude less than the total uncertainty assigned by NBS.

The performance in measuring the reflection coefficient and attenuation has also been checked over 2–17 GHz in 1-GHz steps using procedures similar to those carried out by Hoer at NBS [5]. The results are shown in Figs. 4 and 5 at the representative frequencies of 2, 7, 12, and 17 GHz.

Fig. 4(a) and (b) shows the imprecision in measuring the magnitude and the phase of reflection coefficients of five terminations of nominal VSWR's equal to 1.0, 1.1, 1.2, 2.0, and 'short.' In Fig. 4(c), the consistency represents $||\Gamma_m|-|\Gamma_c||$, where $\Gamma_m$ is the measured reflection coefficient of the attenuator/termination combination, and $\Gamma_c$ is the reflection coefficient calculated from the measured $S$-parameters of the attenuator and the measured reflection coefficient of the termination. There are twenty attenuator/termination combinations out of five terminations of nominal VSWR's equal to 1.0, 1.1, 1.2, 2.0, and 'short,' and four attenuators of nominal attenuations equal to 0, 3, 6, and 10 dB.

Fig. 5(a) and (b) shows the imprecision in measuring the attenuation and phase shift of seven attenuators of nominal attenuations equal to 0, 3, 6, 10, 20, 40, and 60 dB. In Fig. 5(c), the consistency represents the difference between the measured attenuation of two cascaded attenuators and the attenuation calculated from their individually measured $S$-parameters. There are five combinations of 0 dB + 3 dB, 3 dB + 10 dB, 10 dB + 20 dB, 10 dB + 40 dB, and 20 dB + 40 dB.

As shown, the results are not as good as those obtained at NBS for a single frequency [5]. It appears that this is

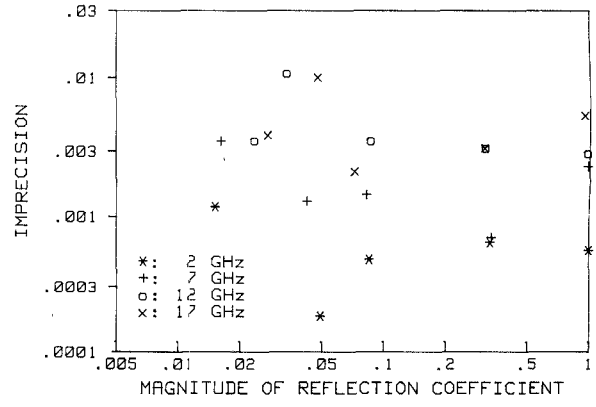


(a)

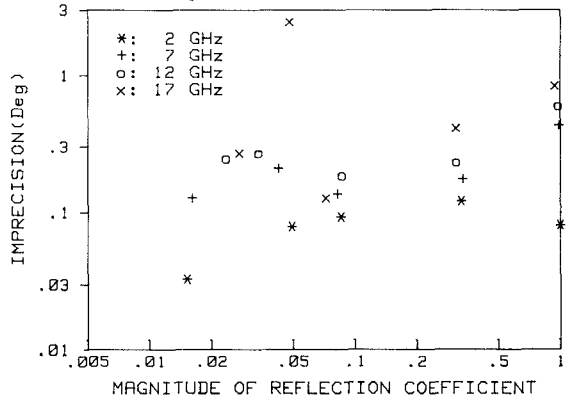


(b)

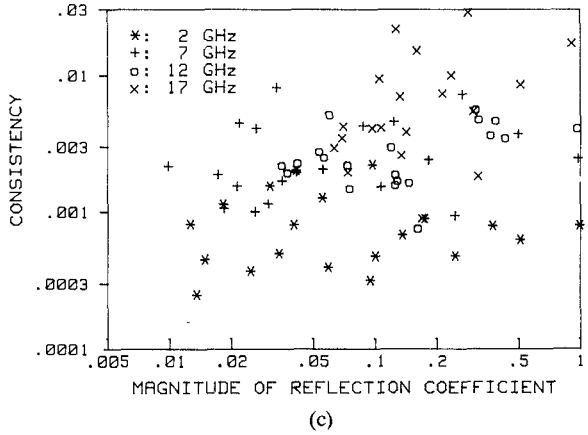


(c)

Fig. 4. Performance in measuring the reflection coefficient. (a) Imprecision in measuring $|\Gamma|$. Standard deviation of five measurements is plotted. (b) Imprecision in measuring the phase of $\Gamma$. Standard deviation in measuring the phase multiplied by the mean value of $|\Gamma|$ is plotted. (c) Consistency in measuring $|\Gamma|$, see text.

partly due to the connector repeatability of the type-$N$, which is worse than that of GR-900 or APC-7. We also observed that the output level of the TWTA's was a little unstable, which have been partly responsible for the results. It is expected that system performances can be considerably improved by changing the connector type of the measurement port and by leveling the output power or

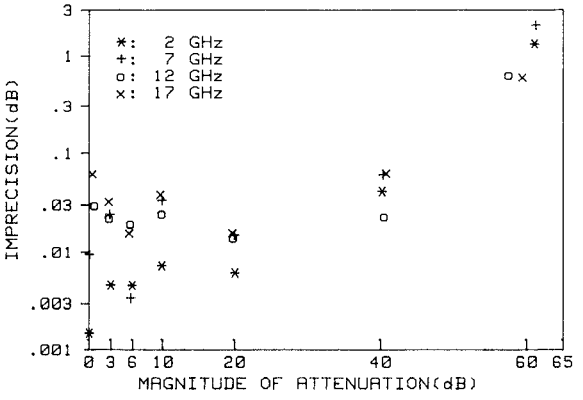


(a)

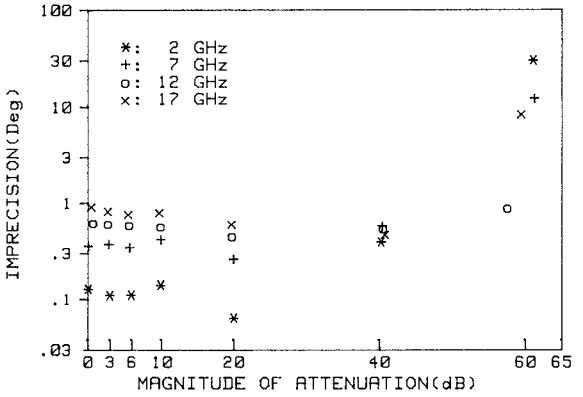


(b)

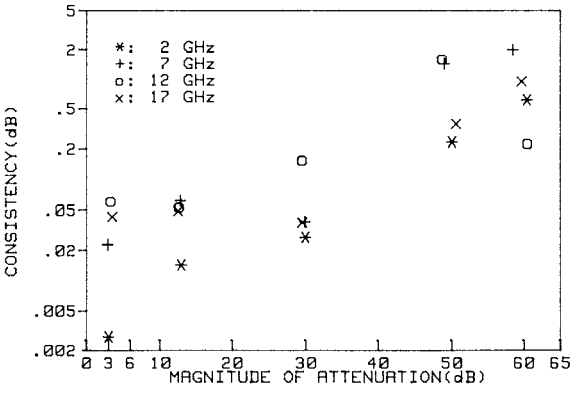


(c)

Fig. 5. Performance in measuring $S$-parameters. (a) Imprecision in measuring attenuation. Standard deviation of five measurements is plotted. (b) Imprecision in measuring phase shift. Standard deviation in measuring the phase is plotted. (c) Consistency in measuring attenuation, see text.

by taking power ratios (i.e., $P_5/P_4$, $P_6/P_4$, etc.) directly with two DVM's, which will eliminate the effect of the power-level fluctuation.

## Acknowledgment

The authors wish to thank C. A. Hoer and Dr. G. F. Engen of NBS for their technical advice throughout the work and for providing us with the NBS software which was the basis of our system software.

## References

[1] G. F. Engen, "An improved circuit for implementing the six-port technique of microwave measurements," *IEEE Trans. Microwave Theory Tech.*, vol. MTT-25, pp. 1080–1083, Dec. 1977.

[2] G. F. Engen and C. A. Hoer, "'Thru-Reflect-Line': An improved technique for calibrating the dual six-port automatic network analyzer," *IEEE Trans. Microwave Theory Tech.*, vol. MTT-27, pp. 987–993, Dec. 1979.

[3] G. F. Engen, "Calibrating the six-port reflectometer by means of sliding terminations," *IEEE Trans. Microwave Theory Tech.*, vol. MTT-26, pp. 951–957, Dec. 1978.

[4] C. A. Hoer, "A network analyzer incorporating two six-port reflectometers," *IEEE Trans. Microwave Theory Tech.*, vol. MTT-25, pp. 1070–1074, Dec. 1977.

[5] C. A. Hoer, "Performance of a dual six-port automatic network analyzer," *IEEE Trans. Microwave Theory Tech.*, vol. MTT-27, pp. 993–998, Dec. 1979.